ELSEVIER

Soil Dynamics and Earthquake Engineering 27 (2007) 414–426

SOIL DYNAMICS AND EARTHQUAKE ENGINEERING

www.elsevier.com/locate/soildyn

Effect of isolation on fragility curves of highway bridges based on simplified approach

Kazi Rezaul Karim[a,*], Fumio Yamazaki[b]

[a]*Department of Civil, Architectural and Environmental Engineering, University of Missouri-Rolla, 326 Butler-Carlton Hall, 1870 Miner Circle, Rolla, MO 65409, USA*

[b]*Department of Urban Environment System, Faculty of Engineering, Chiba University, 1-1-3 Yayoi-cho, Inage-ku, Chiba 263-8522, Japan*

Received 24 October 2005; received in revised form 8 October 2006; accepted 24 October 2006

Abstract

The trend of isolating highway bridges is on the rise after the recent large earthquakes in Japan, the United States, and other countries. Recent investigation shows that isolated systems perform well against seismic forces as the substructures of such systems experience less lateral forces due to energy dissipation of the isolation device. Hence, it is anticipated that there might be an effect on fragility curves of highway bridges due to isolation. In this study, 30 isolated bridge models were considered (and they were designed according to the seismic design code of highway bridges in Japan) to have a wider range of the variation of structural parameters, e.g. pier heights, weights, and over-strength ratio of structures. Then, fragility curves were developed by following a simplified procedure using 250 strong motion records, which were selected from 5 earthquake events that occurred in Japan, the USA, and Taiwan. It is observed that the level of damage probability for the isolated system is less than that of the non-isolated one for a lower level of pier height. However, having the same over-strength ratio of the structures, the level of damage probability for the isolated system is found to be higher for a higher level of pier height compared to the one of the non-isolated system. The proposed simple approach may conveniently be used in constructing fragility curves for a class of isolated bridge structures in Japan that have similar characteristics.

Keywords: Strong motion records; Highway bridges; Dynamic analyses; Fragility curves

1. Introduction

Fragility curves are regarded to be useful tools for estimating the extent of probable damages (slight, moderate, extensive, and complete) of structures due to an earthquake [1–4]. It shows the probability of structure damages as a function of ground motion indices, e.g. peak ground acceleration (PGA) and peak ground velocity (PGV). They allow estimating a damage level for a known ground motion index.

Yamazaki et al. [1] developed a set of empirical fragility curves for highway bridges based on actual damage data from the 1995 Kobe earthquake. However, the type of structure, structural performance (static and dynamic) and variation of input ground motions were not considered in the empirical approach. It is assumed that structural parameters and input motion characteristics (e.g. frequency contents, phase, and duration) have influence on the damage of structures for which there will be an effect on fragility curves.

The present authors [5] developed a set of analytical fragility curves for highway bridge piers based on numerical simulation considering the variation of input ground motions. It was found that there is a significant effect of earthquake ground motions on fragility curves. They also developed a simplified method [6] to construct the fragility curves of non-isolated highway bridges considering the variation of both input ground motions and structural parameters. It was also found that there is a significant effect of both earthquake ground motions and structural parameters on fragility curves.

The trend of isolating highway bridges is on the rise after the recent damaging earthquakes in Japan, the United

*Corresponding author. Tel.: +1 573 341 4479; fax: +1 573 341 4729.
E-mail address: krk2q4@umr.edu (K.R. Karim).

0267-7261/$ - see front matter © 2006 Elsevier Ltd. All rights reserved.
doi:10.1016/j.soildyn.2006.10.006

States, and other countries. Recent investigation shows that isolated systems perform well against seismic forces as the substructures of such systems experience less lateral forces due to energy dissipation of the isolation device [7]. Hence, it is anticipated that there might be an effect on fragility curves of highway bridges due to isolation; in other words, fragility curves for non-isolated bridges may not be applicable to predict the extent of probable damages for isolated systems since the fragility curves of the two systems might be different.

The purpose of this study is to develop fragility curves for isolated bridges by following a simplified procedure [6], and to compare them with the ones of the non-isolated systems. In this objective, 30 isolated bridge models are considered (and they to designed according were the seismic design code of highway bridges in Japan) to have a wider range of the variation of structural parameters, e.g. pier heights, weights, and over-strength ratio of structures. A total of 250 strong motion records are considered as the input motions, which were selected from 5 earthquake events that occurred in Japan, the USA, and Taiwan. Then, using the selected input motions and isolated bridge models, fragility curves are obtained with respect to ground motion parameters by following a simplified approach [6].

2. Development of fragility curves

2.1. Empirical fragility curves

Yamazaki et al. [1] developed a set of empirical fragility curves based on actual damage data from the 1995 Kobe earthquake, and showed the relationship between the damages that occurred to the expressway bridge structures and the ground motion indices. In this approach, the damage data of the expressway structures due to the Kobe earthquake were collected, and the ground motion indices along the expressways were estimated based on the estimated strong motion distribution using Kriging technique. The damage data and ground motion indices were related to each damage rank, and the damage ratio for each damage rank was obtained. Finally, using the damage ratio for each damage rank, the empirical fragility curves for the expressway bridge structures were constructed assuming a lognormal distribution [1,8].

2.2. Analytical fragility curves

The present authors [5] developed a set of analytical fragility curves for highway bridge piers based on numerical simulation and considering the variation of input ground motions. The procedures adopted to construct the analytical fragility curves are briefly described below.

In this approach, first, the non-linear static pushover analysis of the structure is performed [9,10], which includes the shear vs. strain and moment vs. curvature analyses of the cross-sections (it is recommended in the highway bridge design code in Japan [11] that a pier should be divided at least into 50 slices), and the force–displacement relationship at the top of the bridge pier is obtained by using the shear vs. strain and moment vs. curvature relationships of all cross-sections. Using the elastic stiffness (obtained from the force–displacement relationship), the non-linear dynamic response analyses [12] are performed for the selected input ground motions, which are normalized to different excitation levels.

The damage to the structure (pier) is then quantified by a damage index (DI) that is obtained by using a damage model [13] and the number of occurrence of a particular damage rank is counted by calibrating [14] the damage indices in different excitation levels, which is used to obtain the damage ratio of each damage rank in each excitation level. The damage ratio is then plotted on a lognormal probability paper [1,5] from where the two parameters of the fragility curves, i.e., mean and standard deviation are obtained by performing a linear regression analysis. Finally, fragility curves are constructed for each damage rank with respect to the ground motion indices using the obtained mean and standard deviation. The procedures adopted for constructing the analytical fragility curves can be summarized as follows:

1. Selection of the earthquake ground motion records.
2. Normalization of PGA of the selected records to different excitation levels.
3. Making a physical model of the structure.
4. Performing a non-linear static pushover analysis and obtaining the elastic stiffness of the structure.
5. Selection of a hysteretic model for the non-linear dynamic response analysis.
6. Performing the non-linear dynamic response analysis using the elastic stiffness and the selected records.
7. Obtaining the damage indices of the structure in each excitation level using a damage model.
8. Calibration of the damage indices for each damage rank to obtain the damage ratio in each excitation level.
9. Plotting the damage ratio in each excitation level on a lognormal probability paper and obtaining the mean and standard deviation of the fragility curves for each damage rank by performing a linear regression analysis.
10. Construction of fragility curves using the obtained mean and standard deviation with respect to the ground motion indices for each damage rank assuming a lognormal distribution.

2.3. Simplified approach to develop fragility curves

The present authors [6] also developed a simplified method to construct fragility curves for non-isolated bridges based on the observed correlation between the fragility curve parameters and structural parameters. The

procedure adopted to develop the simplified expressions of fragility curves is briefly described below while the details can be found somewhere else [6].

In this approach, first, the fragility curve parameters mean λ and standard deviation ξ are obtained by performing a series of both non-linear static pushover and dynamic response analyses. Then, the relationships between mean λ and standard deviation ξ with the over-strength ratio θ [6,11] are obtained considering all the data points without making any subgroups. The relationships are also obtained by making the data points into some subgroups, for instance, data points for different codes, pier heights, weights, etc. It is observed that λ and θ shows higher correlation for the data points of each level of pier height. Based on this observation, λ for different levels of pier heights are obtained by fixing some θ using the relationships between λ and θ that are obtained for different levels of pier heights. Then, the relationship between λ and h is obtained using the following regression model:

$$\lambda_h = b_0 + b_1 h + b_2 h^2, \tag{1}$$

where λ_h is the mean with respect to h, h the height of the pier, and b_0, b_1 and b_2 are the regression coefficients. Like the data points for each level of pier height, it is also found that there is a strong correlation between λ and h for different θ. It is also observed that the relationships between λ and h obtained for different θ are quite parallel, which implies that knowing only one of the relationships between λ and h for a given θ, the other relationships for different θ can also be obtained knowing only some scale factors for a change of θ. In this objective, the scale factors are obtained for changing different θ for different pier heights considering the relationship between λ and h obtained for a θ equal to 1.0, and the scale factor F_θ is given as

$$F_\theta = a_0 + a_1 \Delta\theta, \tag{2}$$

where F_θ is the scale factor with respect to the change of θ, $\Delta\theta$ the change of θ given as $(\theta-1)$, and a_0 and a_1 are the regression coefficients. Although, the scale factors for different levels of pier heights are found to be very similar, however, to minimize the error that might results for different levels of pier heights, the average scale factor obtained for different pier heights is considered [6]. Hence, the λ value can readily be obtained using Eq. (1) for a known h, and then simply multiplying it by the scale factor F_θ of Eq. (2) that can be obtained for a known $\Delta\theta$. In other words, the λ value can be obtained by using the following expression:

$$\lambda = \lambda_h F_\theta. \tag{3}$$

Substituting for λ_h and F_θ from Eqs. (1) and (2) into Eq. (3) gives

$$\lambda = [b_0 + b_1 h + b_2 h^2][a_0 + a_1 \Delta\theta]. \tag{4}$$

Similar procedure has also been adopted to obtain the expression for standard deviation ξ and the expression for ξ is given as

$$\xi = [b_0 + b_1 h + b_2 h^2][a_0 + a_1 \Delta\theta]. \tag{5}$$

It should be noted that the regression coefficients of Eq. (4) are different than that of Eq. (5), however, same symbols are used for simplicity. It should also be noted that the expressions of fragility curve parameters mean λ and standard deviation ξ given in Eqs. (4) and (5), respectively, hold true for all damage ranks, i.e. slight, moderate, extensive, and complete with respect to both PGA and PGV. Another point also has to be noted that to perform regression analysis and to obtain regression coefficients b_0, b_1, b_2, a_0 and a_1 of Eqs. (4) and (5), fragility curve parameters mean λ and standard deviation ξ are obtained by following the same procedures given in the preceding section, i.e. "analytical fragility curves" section, which provides the foundation for developing the simplified method to obtain the expressions of fragility curve parameters [6].

3. Bridge models

3.1. Description of bridge models

In order to obtain simplified expressions of fragility curve parameters for isolated bridges, a total of 30 bridge models are considered to have a wider range of the variation of structural parameters, and they were designed [15] according to the seismic design code of highway bridges in Japan [11]. For the selected bridge models, the piers are considered rectangular and fixed to the base [16], and a lead–rubber bearing (LRB) is considered as the isolation device [7,16,17]. The ground condition is considered as type II, the regional class is considered as A, and the standard lateral force coefficient k_{hco} is considered as type II [6,11].

The bridge models are divided into three categories, viz. bridges designed with different years' seismic codes, bridges having different pier heights, and bridges having different span lengths or weights, however, the number of spans for the all-bridge models is assumed to be four. The substructures (piers) for any typical bridge model are considered to be similar, in other words, one pier model can be considered as the representative of all other piers for a particular bridge structure. This assumption is adopted to avoid a rigorous computation necessary to perform non-linear pushover analyses for the all piers of a particular bridge model. It should be noted that the non-linear pushover analysis is performed in order to obtain the elastic stiffness of the substructure. The physical model is considered as the one shown in Fig. 1 and the analytical model is shown at the right side of the physical model. It can be seen (Fig. 1) that the analytical model consists of a portion of superstructure, the isolation device (LRB) and the substructure (pier). Since the main concern is the damage of the pier, therefore, this simple analytical model

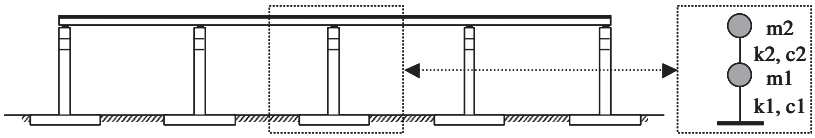

Fig. 1. Physical model of an isolated bridge system used in this study.

Table 1
Structural properties for the 30 isolated bridge models used in this study

Design code	Span length, $L = 30$ and 40 m ($w = 500$ kN/m)										Reinforcement	
	Pier height (m)											
	6		9		12		15		18		Long.	Tie
	Section		Section		Section		Section		Section		ρ_l (%)	ρ_t (%)
	a^a	b^b	a^a	b^b	a^a	b^b	a^a	b^b	a^a	b^b	Area ratio	Vol. ratio
1964	2.0	2.8	2.6	3.2	3.0	3.5	3.4	3.8	3.5	4.0	1.21	0.09
1980	2.1	3.0	2.8	3.2	3.2	3.8	3.8	4.0	3.8	4.2	1.25	0.32
1995	2.2	3.0	2.8	3.4	3.2	4.0	3.8	4.2	4.0	4.5	1.36	1.03

σ'_c (MPa) and σ_{sy} (MPa) are taken as the same for the all codes, and they are taken as 27 and 300, respectively.
[a]Dimension in the longitudinal direction in m.
[b]Dimension in the transverse direction in m.

is adopted in this study, which suffices to see how the bridge pier behaves with an isolation device under seismic loading. It should be noted that if one is interested to see the behaviour of several other components (e.g. failure of deck, cap beam, piles, abutment, etc.) of a particular bridge structure, then a fancy model can be adopted based on any commercially available FEM based software for instance SAP2000 [10], however, that is not the purpose of this study.

Table 1 shows all the structural properties for different categories of bridges having span length of 30 and 40 m with superstructure weight as 500 kN/m. Note that same structural properties have been considered for the all-bridge models having a span length of 40 m, in other words, changing only the span length or weight of the superstructure while all other parameters being unchanged. It can be seen that the pier cross-section changes for different seismic design codes even having the same height, and it changes from smaller to larger from the 1964 code to the 1995 code. It can also be seen that the pier cross-section also changes due to the changes of pier height even if it is designed with the same seismic code, and it changes from smaller to larger from pier height 6 to 18 m. One can also see that the longitudinal (area ratio) and tie (volumetric ratio) reinforcement also changes for different seismic codes, and the value goes higher from the 1964 code to the 1995 code.

3.2. Isolation device-LRB

Kawashima and Shoji [17] recommended that the yield force of the LRB can be taken as 10–20% weight of the superstructure (W), while Ghobarah and Ali [16] recommended that the yield force of the LRB can be taken as 5% W, which provides a reasonable balance between reduced forces in the piers and increased forces on the abutments. While several options may be considered, however, in this study, the yield force and yield stiffness of the LRB are taken as 5% W and 5% W/mm, respectively. Given the yield force level and the lead yield strength of 10–10.5 MPa [15,16], the number and cross-sectional area of the lead plugs can be designed (Fig. 2). The advantage of LRB is that it has low yield strength and sufficiently high initial stiffness that results in higher energy dissipation [7,15–17].

3.3. Analytical model

The analytical model consists of a portion of superstructure, the isolation device (LRB) and the substructure (pier) of the isolated bridge system, which is modeled as a two-degree-of-freedom (2DOF) system [7,16,17], a bilinear hysteretic model was considered for the both substructure [18] and isolation device [7,15–17], the post-yield stiffness was taken as 10% of the initial stiffness for the both substructure and isolation device [16,17], the damping matrix $\mathbf{C}$ is evaluated by using the Rayleigh damping [12,15], and the damping constant h_i is found by using the following expression [11]:

$$h_i = \frac{\sum_{j=1}^{n} h_j \Phi_{ij}^{\mathrm{T}} \mathbf{K}_j \Phi_{ij}}{\Phi_i^{\mathrm{T}} \mathbf{K} \Phi_i}, \tag{6}$$

where h_j is the equivalent damping constant of element j, Φ_{ij} is the mode vector of element j of the ith vibration mode, $\mathbf{K}_j$ is the equivalent stiffness matrix of element j, Φ_i is the mode vector of the overall structure of the ith vibration

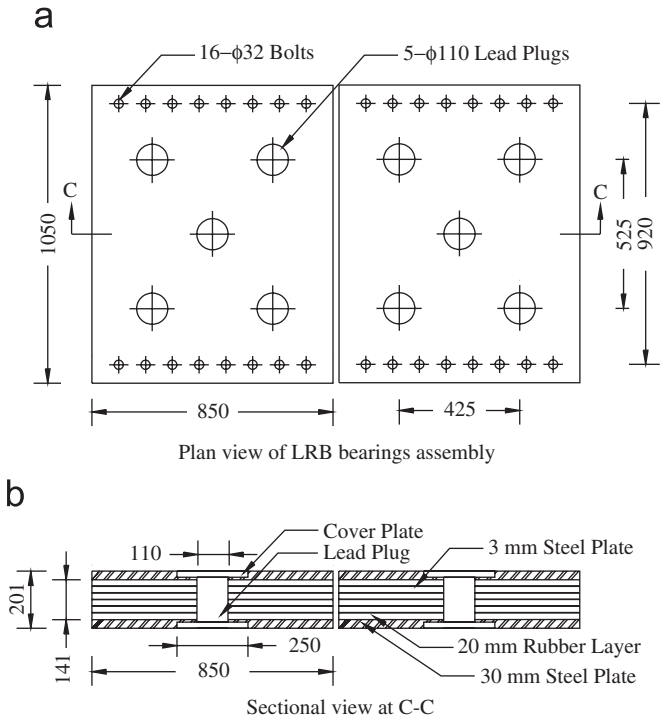

Fig. 2. Details of a lead–rubber bearings (LRB) that can be used as an isolation device for the isolated bridge system. This is an example how the LRB can be designed given the lead yield strength and yield force level [15,16].

mode, and **K** is the equivalent stiffness matrix of the overall structure.

3.4. Displacement and energy demands

Recent investigation shows that isolated systems perform well against seismic forces as the substructures of such systems experience less lateral forces due to energy dissipation of the isolation device [7]. Also, damage to the structure for a given input motion is related to both displacement and energy demands [13]. Hence, it is necessary to see how the displacement and energy demands of isolated systems differ from that of the non-isolated ones.

Fig. 3 shows the plots of displacement and energy histories [19] for the substructure and bearing of an isolated system obtained from the JMA Kobe NS record of the 1995 Kobe earthquake. It can be seen that both the displacement and energy demands of the substructure of the isolated system is less than that of the bearing. Fig. 4 shows the plots of displacement and hysteretic energy demands of the substructures for an isolated and a non-isolated system obtained from the JMA Kobe NS record. One can see that both the displacement and energy demands of the substructure of the isolated system are less than that of the substructure of the non-isolated ones. The lower level of both displacement and energy demands of the substructure of the isolated system than that of the non-isolated ones result due to the energy dissipation of the isolation device [7,16,17], and it implies that the isolated system performs better against seismic forces than the non-isolated system does.

4. Simplified expressions of fragility curve parameters

Fragility curve parameters λ and ξ for the 30 isolated bridge models are obtained by following the same procedure given in the "analytical fragility curves" section [5] using the selected 250 records as the input motions. Then, simplified expressions for both the λ and ξ of Eqs. (4) and (5) are obtained by following the same procedure given in the "Simplified approach to develop fragility curves" section [6]. Fig. 5 shows the graphical representation to obtain the simplified expression for λ for a slight damage with respect to PGA. Fig. 6(a) shows the relationships between λ and θ obtained for different damage ranks with respect to PGA for a θ equal to 1.0, and the corresponding average scale factors for λ obtained for different damage ranks are shown in Fig. 6(b). Finally, the regression coefficients of Eqs. (4) and (5) are obtained for all the damage ranks with respect to both PGA and PGV by performing both linear and nonlinear regression analyses, and the regression coefficients are shown in Table 2. Note that the corresponding R^2 values are also shown in the same table.

4.1. Numerical example

To see how the simplified expressions of fragility curve parameters work, a different bridge structure is considered, which was not used to obtain the simplified expressions. The bridge was designed according to the recent seismic design code for highway bridges in Japan [11]. It is assumed that only the number of spans, span length, superstructure weight, height and cross-section of the pier can be changed while other conditions being the same as that of the 30 bridge models that were used to develop the simplified expressions. For the example bridge structure, the number of spans is assumed to be 5, the length of each span is taken as 50 m, the weight is taken as 320 kN/m, the height of each pier is taken as 8 m, and the cross-section of each pier is taken as 2.5 by 3 m. The over-strength ratio θ is calculated [6,11] as 1.21. Now, knowing the height of the pier as 8 m and θ as 1.21, the fragility curve parameters λ and ξ for different damage ranks with respect to both PGA and PGV are obtained using the simplified expressions given in Eqs. (4) and (5), and using the regression coefficients given in Table 2. λ and ξ are also obtained by performing a series of both nonlinear static pushover and dynamic response analyses.

Table 3 shows the list of the fragility curve parameters for the example bridge structure obtained from both analytical and simplified methods, and the corresponding errors ε for both λ and ξ with respect to the analytical ones are also shown in the same table. Figs. 7 and 8 show the

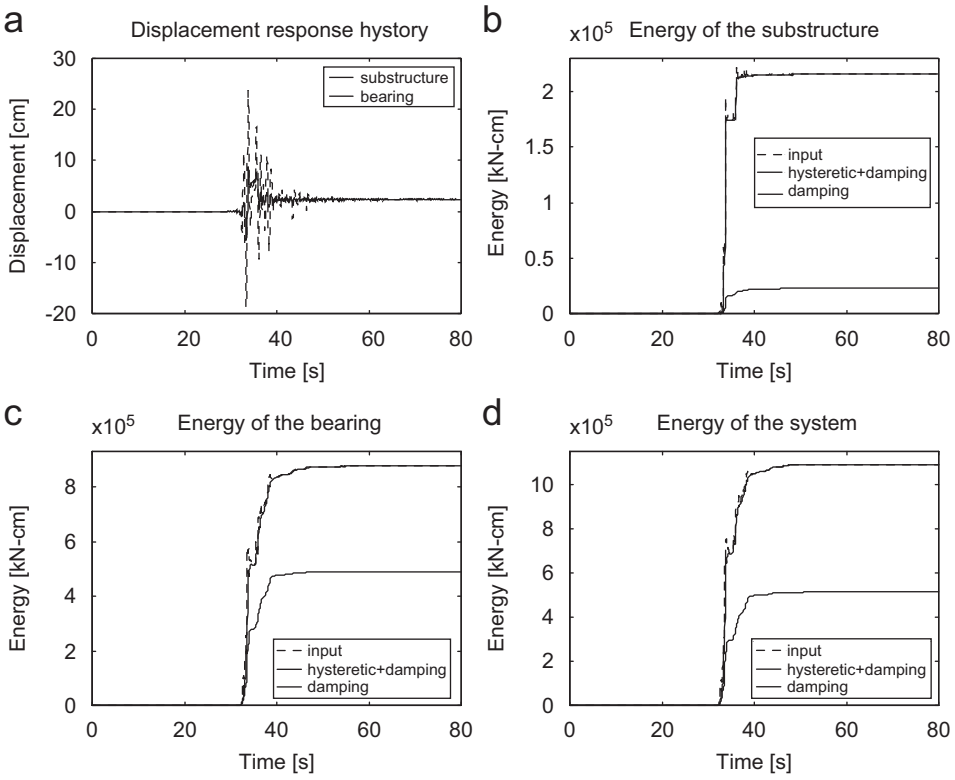

Fig. 3. Displacement and energy histories of an isolated bridge system obtained from the JMA Kobe NS record of the 1995 Kobe earthquake, (a) displacement response histories of the substructure and bearing, (b) energy of the substructure, (c) energy of the bearing, and (d) energy of the system.

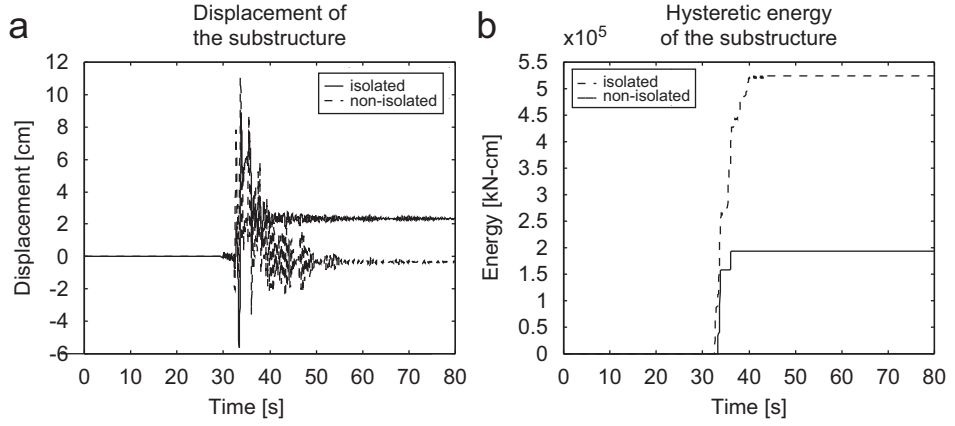

Fig. 4. (a) Displacement response histories, and (b) hysteretic energy of the substructures of an isolated and a non-isolated bridge system obtained from the JMA Kobe NS record of the 1995 Kobe earthquake.

fragility curves for all damage ranks with respect to PGA and PGV, respectively, obtained from both analytical and simplified methods. It can be seen that the fragility curves obtained by both analytical and simplified methods seem to be very close with respect to PGV, however, a very small difference is observed with respect to PGA for the all-damage ranks. Note that the maximum error with respect to both PGA and PGV for both λ and ξ are shown in Table 3 with an underline mark. It can be seen that the maximum error for λ with respect to both PGA and PGV is found to be only 1.8%, and for ξ it is found as 19.8%.

It should be noted that λ controls the amplitude and ξ controls the shape of the fragility curves. The 19.8% error for ξ does not necessarily mean that it might result in a significant effect on the fragility curves, and the evidence can be seen in the fragility curves (Figs. 7 and 8). Hence, the error terms for both λ and ξ given in Table 3 seem to be within an acceptable range, and the simplified method may

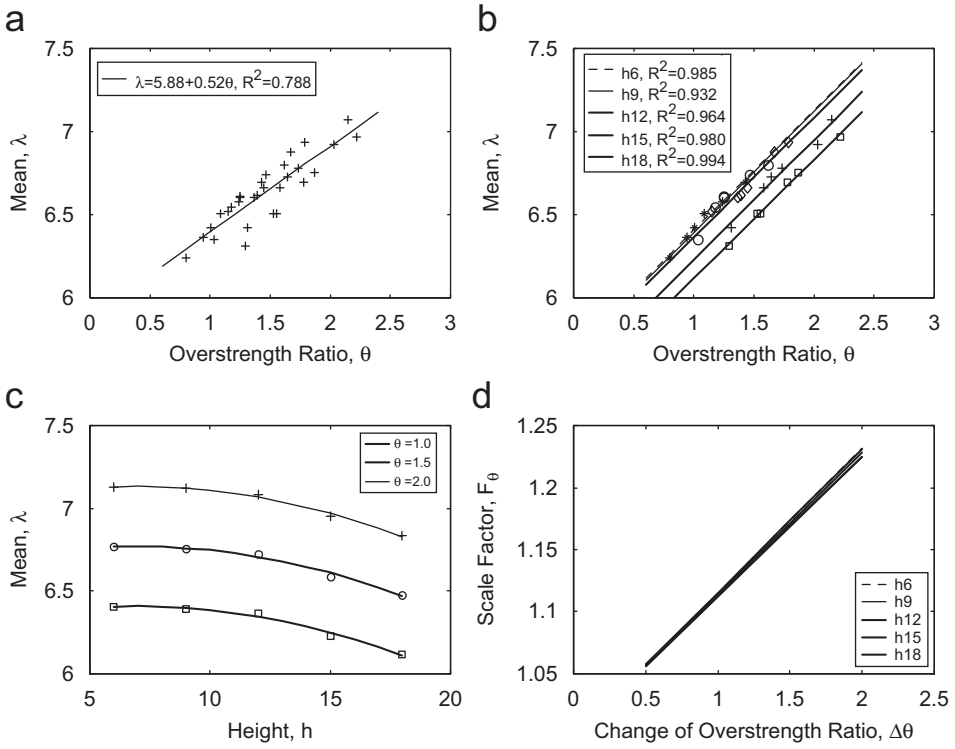

Fig. 5. Relationship between (a) λ and θ obtained for the 30 isolated bridge models used in this study, (b) λ and θ for different pier heights, (c) λ and h for different θ, and (d) F_θ and $\Delta\theta$ for different pier heights, all for a slight damage with respect to PGA.

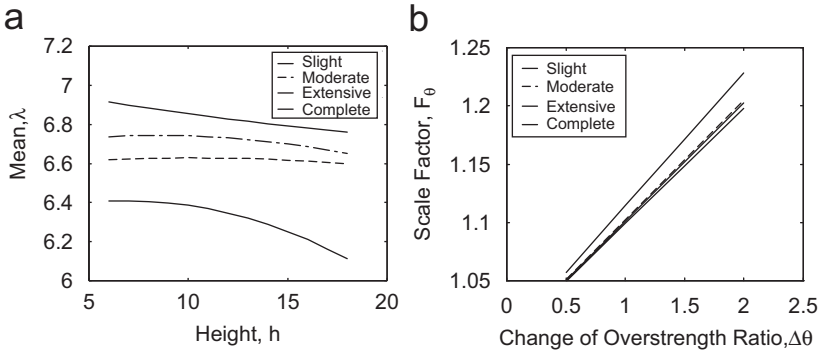

Fig. 6. Relationship between (a) λ and h for θ equal to 1.0, and (b) average F_θ and $\Delta\theta$ obtained for different damage ranks with respect to PGA.

conveniently be used to construct the fragility curves for isolated bridge structures knowing the height h and overstrength ratio θ only. It should be noted that the simplified expressions of fragility curve parameters are obtained based on a set of isolated bridge systems, and these simplified expressions for fragility curve parameters may conveniently be used to construct the fragility curves of similar kind of isolated bridge structures that fall within the same group and have similar characteristics.

5. Fragility curves for both isolated and non-isolated bridges

The present authors [6] also developed simplified expressions to construct fragility curves of non-isolated highway bridges. In this study, following the same procedure, simplified expressions are also developed to construct the fragility curves for isolated highway bridges, which are given in the preceding section. Since simplified expressions show the correlation between the fragility curve parameters and the structural parameters, they might conveniently be used to construct the fragility curves for the both isolated and non-isolated bridges. However, since the two systems are different, it is necessary to see how the fragility curves of both the systems differ from each other based on the simplified expressions.

Fig. 9 shows the plots of the relationship between fragility curve parameter mean λ and pier height h for a θ equal to 1.5 obtained from the simplified method for both

Table 2
List of the regression coefficients for the fragility curve parameters obtained from the simplified method

Indices	DR	Parameters																	
		λ									ξ								
		$\lambda_h = b_0+b_1h+b_2h^2$					$F_\theta = a_0+a_1\Delta\theta$				$\xi_h = b_0+b_1h+b_2h^2$					$F_\theta = a_0+a_1\Delta\theta$			
		b_0	b_1	b_2	σ	R^2	a_0	a_1	σ	R^2	b_0	b_1	b_2	σ	R^2	a_0	a_1	σ	R^2
PGA	S	6.30	0.03	−0.0024	0.022	0.984	1.00	0.11	0.00	1.00	0.40	−0.0006	−0.0006	0.007	0.990	1.00	−0.39	0.00	1.00
	M	6.58	0.01	−0.0005	0.031	0.812	1.00	0.10	0.00	1.00	0.41	0.0002	0.0001	0.012	0.981	1.00	−0.38	0.00	1.00
	E	6.67	0.02	−0.0010	0.017	0.906	1.00	0.10	0.00	1.00	0.27	−0.0008	0.0003	0.015	0.971	1.00	−0.63	0.00	1.00
	C	7.02	−0.02	0.0003	0.047	0.770	1.00	0.10	0.00	1.00	0.38	−0.0043	0.0002	0.002	0.997	1.00	−0.70	0.00	1.00
PGV	S	4.42	0.001	−0.002	0.013	0.998	1.00	0.31	0.00	1.00	0.59	−0.001	−0.0002	0.007	0.967	1.00	0.24	0.00	1.00
	M	4.25	0.091	−0.004	0.036	0.933	1.00	0.26	0.00	1.00	0.59	0.005	−0.0005	0.008	0.978	1.00	0.48	0.00	1.00
	E	4.51	0.080	−0.004	0.016	0.994	1.00	0.29	0.00	1.00	0.63	0.004	−0.0005	0.010	0.969	1.00	0.47	0.00	1.00
	C	489	0.068	−0.003	0.015	0.973	1.00	0.18	0.00	1.00	0.87	−0.034	0.0007	0.011	0.991	1.00	0.67	0.00	1.00

DR: damage rank, S: slight, M: moderate, E: extensive, C: complete.

Table 3
List of the fragility curve parameters for the example isolated bridge structure obtained from both analytical and simplified methods

Indices	DR	Parameters					
		λ			ξ		
		Analytical	Simplified	Error, ε (%)	Analytical	Simplified	Error, ε (%)
PGA	S	6.60	6.56	0.61	0.52	0.51	1.57
	M	6.82	6.77	0.77	0.47	0.45	3.46
	E	6.94	6.89	0.72	0.42	0.41	2.14
	C	7.14	7.03	1.55	0.42	0.34	19.77
PGV	S	4.60	4.57	0.61	0.59	0.60	1.04
	M	4.96	4.96	0.12	0.63	0.66	3.52
	E	5.26	5.16	1.80	0.75	0.69	7.86
	C	5.46	5.43	0.53	0.75	0.73	3.05

DR: damage rank, S: slight, M: moderate, E: extensive, C: complete.

isolated and non-isolated systems for different damage ranks with respect to PGA. Note that the simplified expressions for the non-isolated system were taken from the previous study [6]. It can be seen that the λ for the isolated system is higher than that of the non-isolated one for the all-damage ranks for a lower level of pier height, which implies that the level of damage probability for the isolated system is less than that of the non-isolated one when the level of pier height is not so large. However, one can see that as the pier height changes from lower to a higher level, the mean λ of the isolated system seems to get closer to the non-isolated one, and eventually, in case of extensive and complete damages, it is less than that of the non-isolated one after a certain level of pier height. Similar trend is also found with respect to PGV, and the plots are shown in Fig. 10.

The trend of converging the mean λ of the isolated system with that of the non-isolated one for a higher level of pier height implies that if the pier height of the bridge is very high, for instance, say more than 20 m, then the isolated system may not be so effective. It should be noted that fragility curves are also a function of standard deviation ξ, and both the mean λ and standard deviation ξ are also functions of scale factor F_θ that is obtained for a given over-strength ratio θ. Hence, to see the effect of isolation on fragility curves, it is necessary to construct them for the both isolated and non-isolated systems considering all these factors.

Fig. 11 shows the plots of the fragility curves for the isolated and non-isolated bridges for an extensive damage with respect to PGA obtained from the simplified expressions for different level of pier heights with an over-strength ratio θ equal to 1.5. It can be seen (Figs. 11(a) and (b)) that the level of damage probability for the isolated system is less than that of the non-isolated one for a pier height of 5 and 10 m, respectively, and its damage level seems to be similar to that of the non-isolated one when the pier height is 15 m (Fig. 11(c)). Now, if one looks at

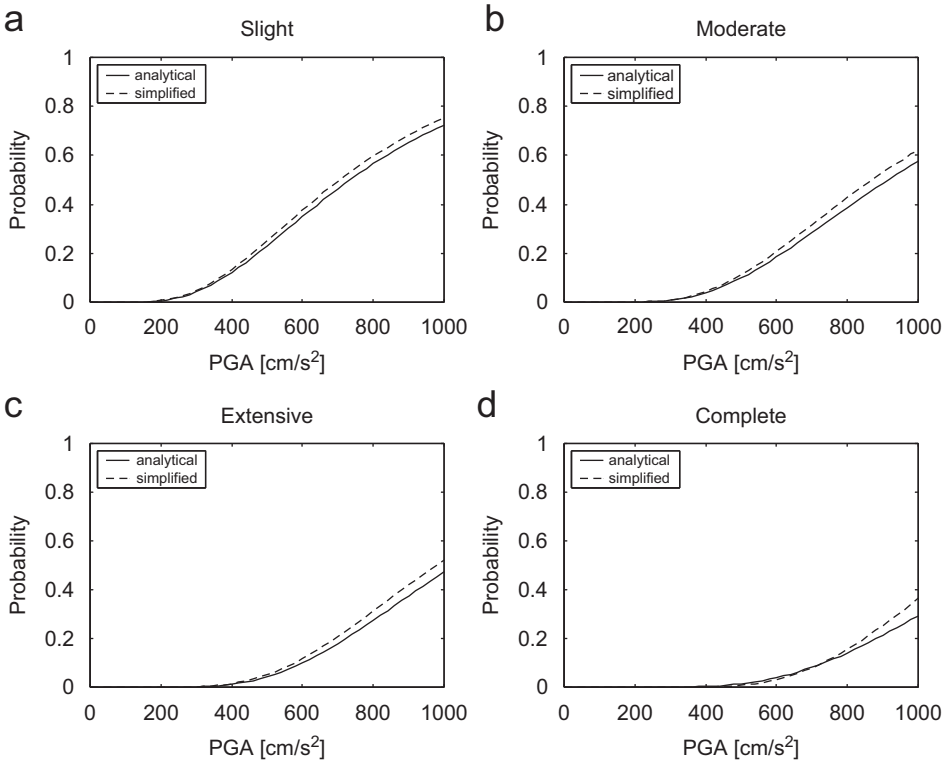

Fig. 7. Comparison of the fragility curves obtained from both analytical and simplified methods for an isolated bridge system with respect to PGA.

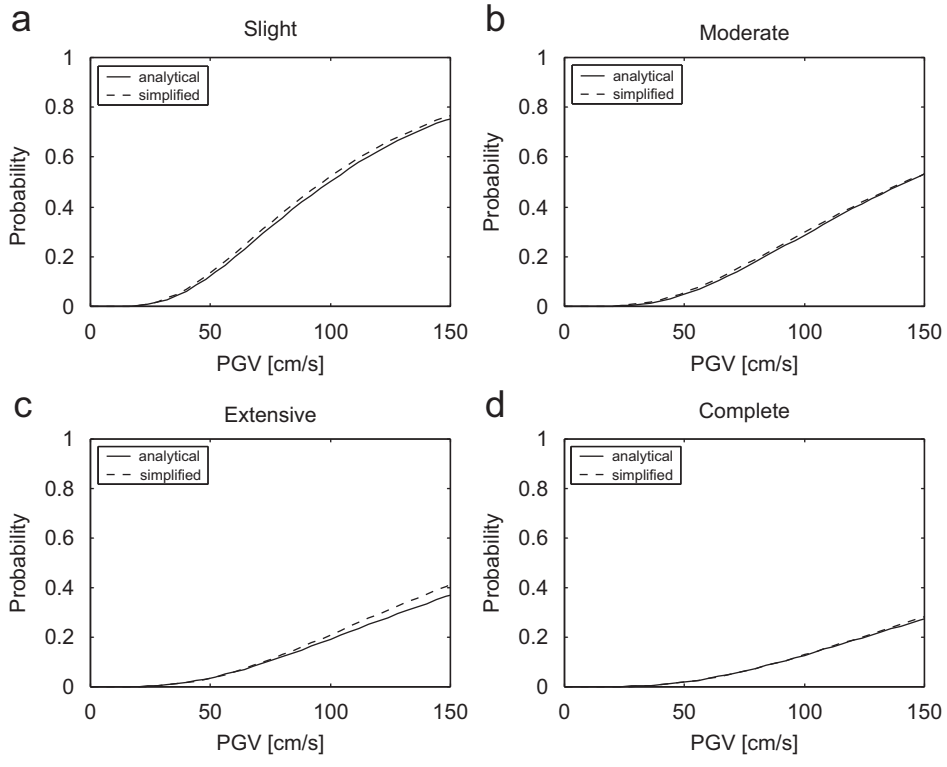

Fig. 8. Comparison of the fragility curves obtained from both analytical and simplified methods for an isolated bridge system with respect to PGV.

Fig. 11(d), then it can be seen that the level of damage probability for the isolated system is higher than that of the non-isolated one where the pier height is 20 m. Similar trend is also observed on the fragility curves obtained for both isolated and non-isolated systems with respect to PGV, and the plots are shown in Fig. 12.

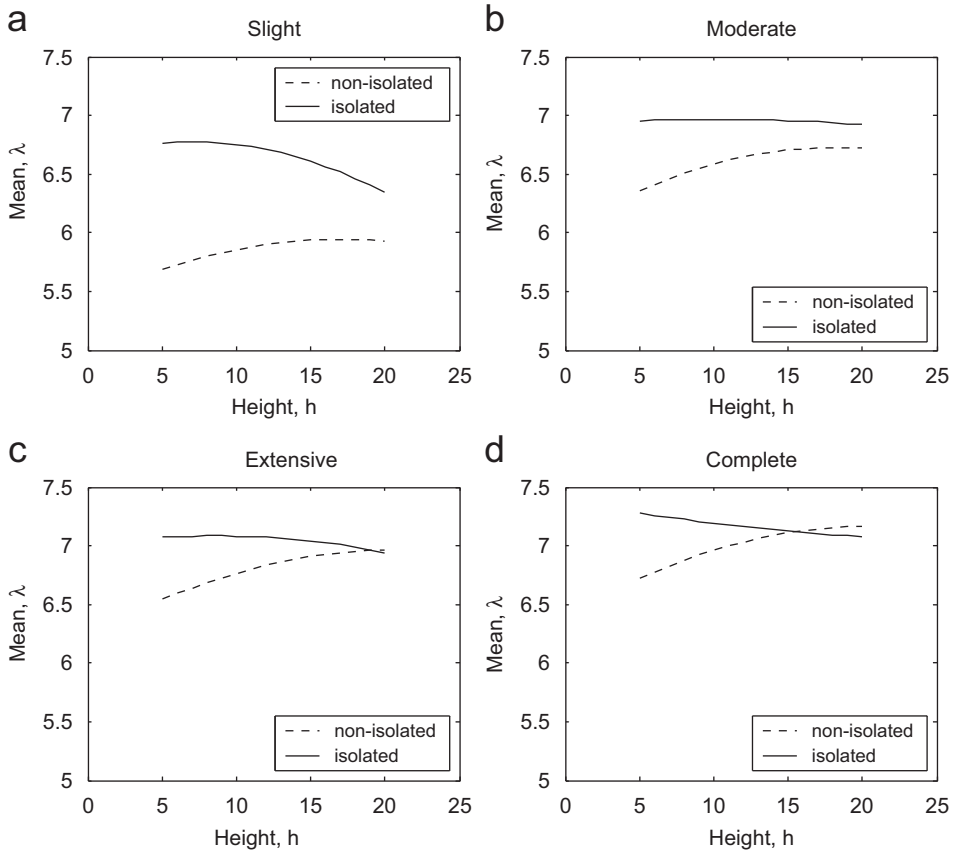

Fig. 9. Comparison of the relationship between λ and h for θ equal to 1.5 obtained from the simplified method for the isolated and non-isolated bridge systems for different damage ranks with respect to PGA.

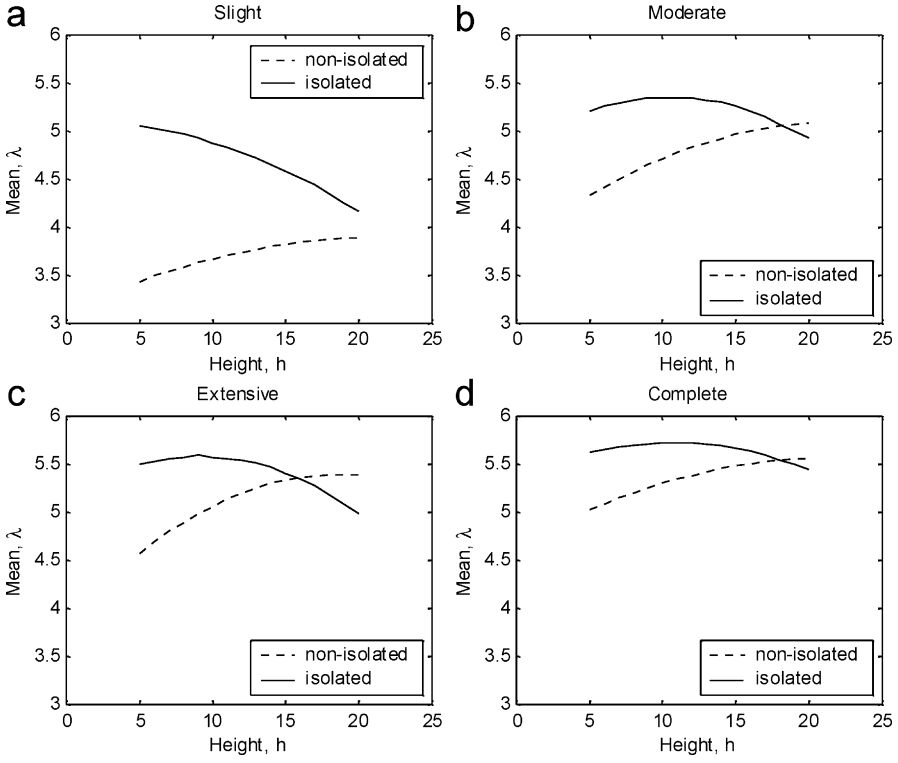

Fig. 10. Comparison of the relationship between λ and h for θ equal to 1.5 obtained from the simplified method for the isolated and non-isolated bridge systems for different damage ranks with respect to PGV.

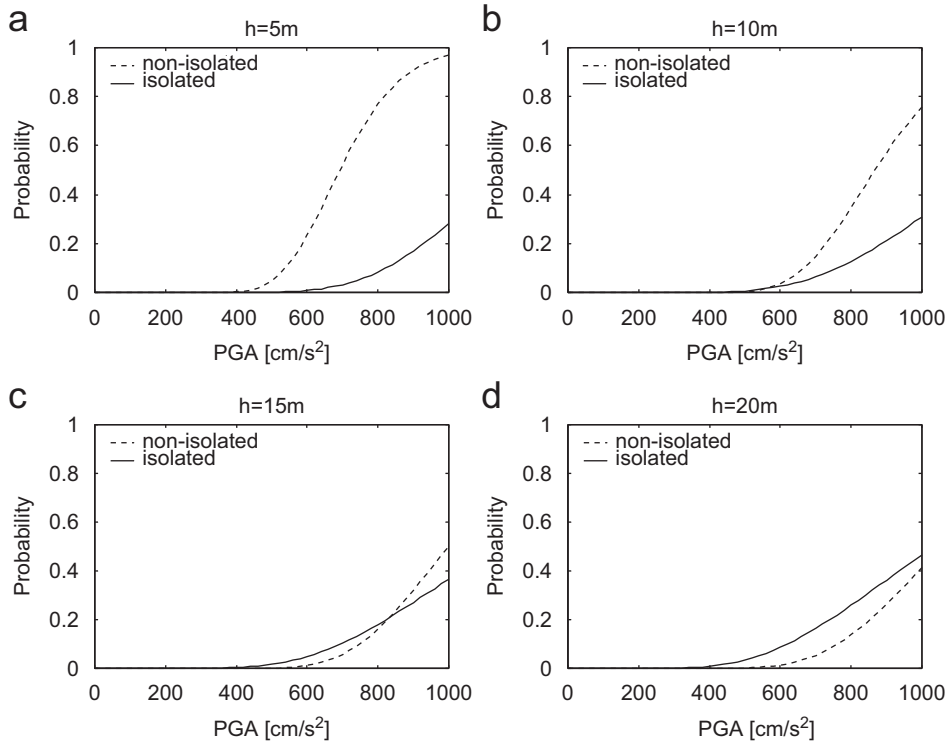

Fig. 11. Comparison of the fragility curves for the isolated and non-isolated bridge systems with respect to PGA obtained from the simplified method for different pier heights, all for an extensive damage with θ equal to 1.5.

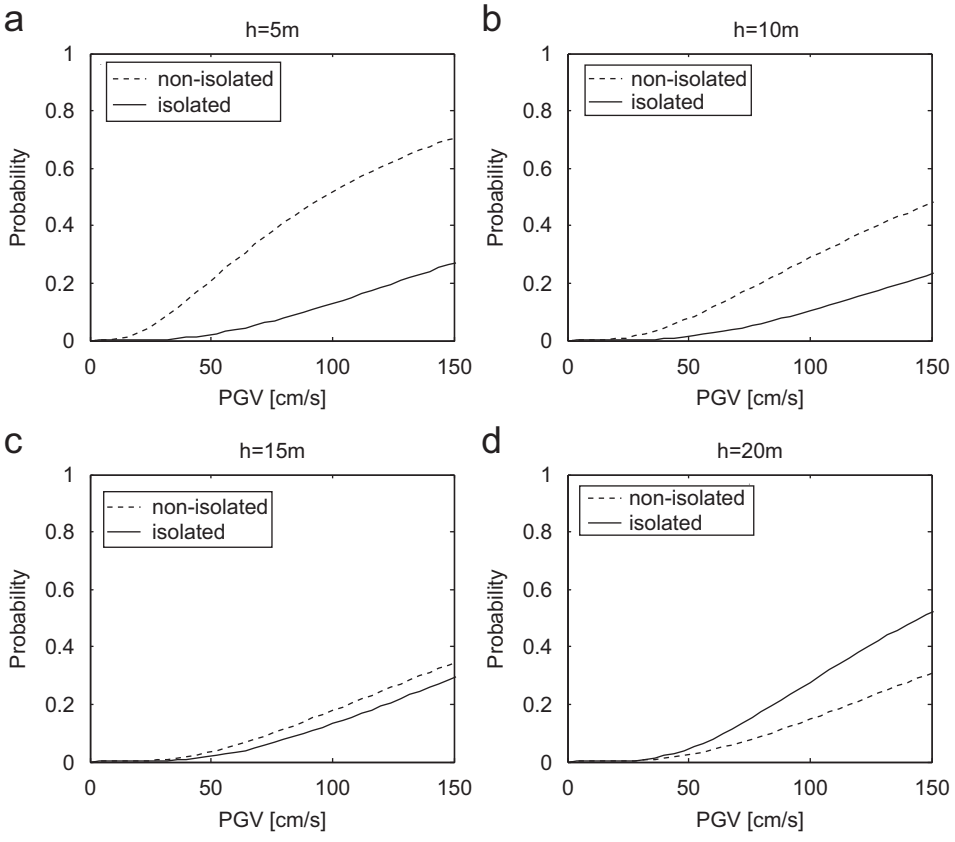

Fig. 12. Comparison of the fragility curves for the isolated and non-isolated bridge systems with respect to PGV obtained from the simplified method for different pier heights, all for an extensive damage with a θ equal to 1.5.

Note that the over-strength ratio θ is considered being the same for all levels of pier heights, and it is taken as 1.5. It means that when the pier height is to be higher then even having the same over-strength ratio, the level of damage probability for the isolated system goes higher compared to the one of the non-isolated system. Several factors may be addressed in this regard. Firstly, simple expressions are obtained for a limited range of pier heights, i.e. 6 to 18 m, which may imply that the simple expressions are valid only for the said range of pier heights. Secondly, the strength for the isolation device is considered as the same (5% W) for the all level of pier heights, which may underestimate the energy dissipation of the isolation device for a higher level of pier heights. Thirdly, due to the elongation of the natural period, the pier with more height become less stiff (i.e. more flexible) compared to the one with less height. This observation is supported with the fact that an isolation device is more effective for a stiff structure and it turns out to be very less effective for a flexible structure. Finally, the failure of the isolation device is not considered in this study, which may have some effect on the fragility curves for a higher level of pier height.

Although, the soil–structure interaction (SSI) effect is generally not so severe for non-isolated bridge structures except for the case with strong soil non-linearity, isolated bridges are regarded to be more susceptible to the effect of SSI during an earthquake [20]. Thus, it is anticipated that there might be an effect on the fragility curves of isolated bridges due to SSI; hence, a further study is recommended in this regard. Also, several other factors should be kept in mind, for instance, different design codes in other countries, several other components of bridge structures (e.g. failure of deck, cap beam, piles, abutment, etc.), different seismic zones, different soil conditions, etc. While the present study considers only a few of them (e.g. failure of bridge pier, seismic zone A, soil type II, lateral force coefficient of type II, Japanese seismic design code for highway bridges, etc.), however, same simple approach can be adopted in deriving the simple expressions for fragility curve parameters of isolated bridge structures considering all the parameters or a combination of several parameters.

6. Conclusions

Simple expressions of fragility curve parameters for isolated highway bridge structures were obtained based on numerical simulation with respect to the ground motion parameters using 250 strong motion records. Fragility curves for the both isolated and non-isolated systems were also constructed based on the obtained simplified expressions and using the seismic design code of highway bridges in Japan.

It was observed that the level of damage probability for the isolated system is less than that of the non-isolated one for a lower level of pier height. However, having the same over-strength ratio of the bridges, the level of damage probability for the isolated system is found to be higher for a higher level of pier height compared to the one of the non-isolated system. It implies that the level of damage probability for the isolated systems tends to be higher for a higher level of pier height. This might be due to fact that the failure of the isolation device was not considered in the present study as well as the strength of the isolation device was considered as the same for the all level of pier heights. In other words, the fragility curves may differ from the one where the failure of the isolation device as well as different level of strengths of the isolation device for different level of pier heights would have been considered.

The simple expressions may be a very useful tool, and may conveniently be used to construct the fragility curves for isolated bridges in Japan that fall within the same group and have similar characteristics. However, it is anticipated that the simple expressions of fragility curves developed in this study may not be applicable for the isolated systems that have SSI effect, and a further research is recommended in this regard. Also, the same simple expressions may not be applicable for other countries since it is based on only Japanese seismic design code, however, the same simple approach may be adopted in constructing the fragility curves using different seismic codes of other countries.

Acknowledgements

The authors would like to thank the editor and the anonymous reviewers who spent their valuable time in reviewing this paper. Their valuable comments in modifying this paper is highly appreciated.

References

[1] Yamazaki F, Motomura H, Hamada T. Damage assessment of expressway networks in Japan based on seismic monitoring. In: Proceedings of the 12th world conference on earthquake engineering. 2000, Paper no 0551 [CD-ROM].

[2] Basoz N, Kiremidjian AS. Evaluation of bridge damage data from the Loma Prieta and Northridge, CA earthquakes. Report no 127, The John A. Blume Earthquake Engineering Center, Department of Civil Engineering, Stanford University, 1997.

[3] Mander JB, Basoz N. Seismic fragility curves theory for highway bridges. In: Proceedings of the fifth US conference on lifeline earthquake engineering. TCLEE no 16, ASCE, 1999. pp. 31–40.

[4] Kircher CA, Nassar AA, Kustu O, Holmes WT. Development of building damage functions for earthquake loss estimation. Earthquake Spectra 1997;13(4):663–82.

[5] Karim KR, Yamazaki F. Effect of earthquake ground motions on fragility curves of highway bridge piers based on numerical simulation. Earthquake Eng Struct Dyn 2001;30(12):1839–56.

[6] Karim KR, Yamazaki F. A simplified method of constructing fragility curves for highway bridges. Earthquake Eng Struct Dyn 2003;32(10):1603–26.

[7] Chaudhary MTA, Abe M, Fujino Y, Yoshida J. System identification and performance evaluation of two base-isolated bridges using seismic data. Journal of Structural Eng ASCE 2000;126(10):1187–96.

[8] Sucuoglu H, Yucemen S, Gezer A, Erberik A. Statistical evaluation of the damage potential of earthquake ground motions. Struct Saf 1999;20(4):357–78.

[9] Bentz EC, Collins MP. Response-2000. Software program for load–deformation response of reinforced concrete section. 〈http://www.ecf.utoronto.ca/~bentz/inter4/inter4.shtml〉, 2000.
[10] SAP2000. Integrated structural analysis and design software. Computers and Structures Inc.; 2000.
[11] EED. Design specifications of highway bridges. Part V: seismic design. Technical memorandum of EED, PWRI, no 9801, 1998.
[12] Chopra AK. Dynamics of structures: theory and application to earthquake engineering. Upper Saddle River, NJ: Prentice-Hall; 1995.
[13] Park YJ, Ang AH-S. Seismic damage analysis of reinforced concrete buildings. J Struct Eng ASCE 1985;111(4):740–57.
[14] Ghobarah A, Aly NM, El-Attar M. Performance level criteria and evaluation. In: Proceedings of the international workshop on seismic design methodologies for the next generation of codes. Balkema, Rotterdam, 1997. p. 207–15.
[15] Priestley MJN, Seible F, Calvi GM. Seismic design and retrofit of bridges. New York: Wiley; 1996.
[16] Ghobarah A, Ali HM. Seismic performance of highway bridges. Eng Struct 1988;10:157–66.
[17] Kawashima K, Shoji G. Interaction of hysteretic behavior between isolator/damper and pier in an isolated bridge. J Struct Eng-JSCE 1998;44A:213–21.
[18] Kawashima K, Macrae GA. The seismic response of bilinear oscillators using Japanese earthquake records. J Res, PWRI, Ministry of Construction, Japan 1993;30:7–146.
[19] Uang C-M, Bertero VV. Evaluation of seismic energy in structures. Earthquake Eng Struct Dyn 1990;19:77–90.
[20] Chaudhary MTA, Abe M, Fujino Y. Identification of soil–structure interaction effect in base-isolated bridges from earthquake records. Soil Dyn Earthquake Eng 2001;21(8):713–25.